Available online at www.sciencedirect.com
ScienceDirect
Journal of Volcanology and Geothermal Research xx (2008) xxx–xxx
Journal of volcanology and geothermal research
www.elsevier.com/locate/jvolgeores

Research paper

On the dynamics of volcanic columns: A comparison of field data with a new model of negatively buoyant jets

G. Carazzo *, E. Kaminski, S. Tait

Equipe de Dynamique des Fluides Géologiques, IPG Paris and Université Paris-Diderot, CNRS, 4 place Jussieu, 75252 Paris cédex 05, France

Received 29 May 2007; accepted 9 January 2008

Abstract

Explosive volcanic eruptions propel high-velocity turbulent jets into the atmosphere and are one of the most powerful and dangerous turbulent flows on Earth. Such eruptions are particularly difficult to predict due to their unusual dynamics that allow the jet to form a high buoyant Plinian plume or dense pyroclastic flows when the column collapses. A major goal of physical volcanology has been to predict quantitatively the limit between the flow regimes, as a function of exit conditions specified at the vent, which requires a physical model constrained by geologic field data. A first generation of quasi-analytic models, developed over 20–30 years although qualitatively successful, has failed to achieve this goal, because they overestimate by more than one order of magnitude the mass flux at the transition. There has been no consensus on whether this mostly reflects poor knowledge of geologic parameters or inadequacies in the physical description of the dynamics. Direct numerical simulations bring considerable advances in the study of unsteady phenomena that occur within the volcanic column, but their complexity makes the deciphering of the underlying dynamics challenging. Here, we present a basis for a new generation of 1D-models that includes a more sophisticated description of the rate of entrainment of air into the jet as a function of its buoyancy. In this framework, we demonstrate that the inconsistency between previous 1D models and field data is due to the omission of a key ingredient in the modeling of turbulence: reduction of entrainment due to the high density of the volcanic jet. We show that negative buoyancy near the base of the jet reduces the coefficient governing turbulent mixing to much less than the value commonly assumed based on experimental studies of neutrally buoyant jets and positively buoyant plumes. The results of our new model, allowing for variable entrainment as a function of local Richardson number, greatly improve the quantitative prediction of the transition as constrained by field data from a large number of eruptions.

Keywords: Plinian column; pyroclastic flows; turbulent entrainment; tephra deposits

1. Introduction

Quantitative prediction of the behavior of explosive eruption columns is a major challenge for physical volcanology. The remarkable fluid dynamics of these dense mixtures of gas and hot particles has come to be characterized in terms of two end-member behaviors: in one, the flow rises high into the atmosphere by natural convection (the "Plinian" regime), in the other it collapses to form pyroclastic flows. These unusual dynamics were initially deduced from the structure of prehistoric deposits (Sparks and Walker, 1977; Druitt et al., 1989) but have now also been confirmed by real-time observation of historical eruptions (Carey et al., 1990; Newhall and Punongbayan, 1991). At the vent, the mixture of gas, solid particles of juvenile and lithic material and droplets of magma has a bulk density greater than the surrounding atmosphere (Fig. 1) and its exit velocity reaches several hundred meters per second (Wilson, 1976). As the volcanic flow rises, cold atmospheric air is entrained by turbulent mixing and heated by the hot pyroclasts. Heat exchanges cause rapid expansion of the gas and a tremendous reduction in the bulk density of the mixture (Sparks and Wilson, 1976; Woods, 1995). At the same time, the flow is strongly decelerating both due to the mixing and because of its negative buoyancy. The Plinian regime occurs when the bulk density of the column attains values below

* Corresponding author.
E-mail address: carazzo@ipgp.jussieu.fr (G. Carazzo).

0377-0273/$ - see front matter © 2008 Elsevier B.V. All rights reserved.
doi:10.1016/j.jvolgeores.2008.01.002

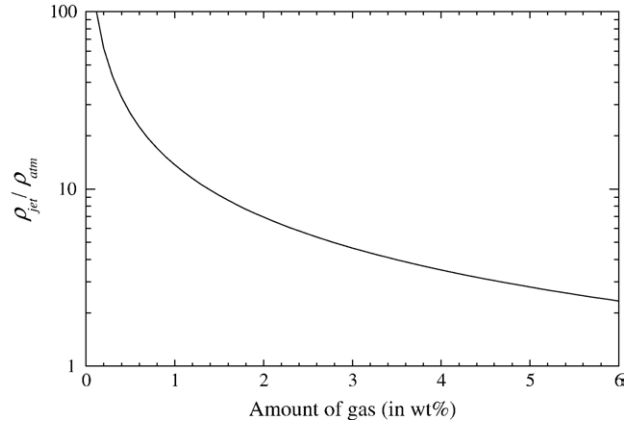

Fig. 1. Ratio of the density of the volcanic mixture (gas+pumice) ρ_{jet} on the atmospheric density at the source ρ_{atm} as a function of the initial amount of gas for a pumice density of 700 kg/m^3, a temperature of 1200 K, and at 1 atm.

atmospheric density before its initial upward momentum has been exhausted. Positive buoyancy then lifts the volcanic cloud by natural convection until it reaches a neutral buoyancy level in the atmosphere and spreads out horizontally typically under the influence of stratospheric winds. The pyroclastic flow regime corresponds to column collapse when the initial momentum is not sufficient to carry the flow up to the point of buoyancy inversion. These different dynamic behaviors often follow one another during a single eruption, and directly influence the nature of hazards. Whereas the powerful energy released by explosive eruptions is dispersed in an extended rain of ash and pumice cooled by heat exchanges when the column reaches the Plinian regime, pyroclastic flows focus all their energy along the ground and remain very hot because collapsing columns mix much less with the atmosphere, increasing their power of destruction. It is thus of crucial importance to better understand the physics of the regime transition in explosive eruptions.

A first generation of quasi-analytical 1D models were developed over 20–30 years to explain column behavior (Wilson, 1976; Sparks, 1986; Woods, 1988). These models, based on the representation of the volcanic mixture by a single "equivalent" phase, clarified the main parameters controlling the Plinian plume dynamics. In particular, they identified the different dynamics of the basal and convective regions of the column and the mechanisms governing the transport and the sedimentation of pyroclasts. In parallel to these studies, laboratory experiments were designed to reproduce volcanic columns (Carey et al., 1988; Woods and Caulfield, 1992; Woods and Bursik, 1994) and gave results qualitatively consistent with the theoretical models.

Since the 1990s, sophisticated numerical 2D and 3D models of multiphase compressible flows have been developed with an aim of clarifying the complex processes occurring in the column (Valentine and Wohletz, 1989; Valentine et al., 1991; Neri and Dobran, 1994; Neri and Macedonio, 1996; Oberhuber et al., 1998; Neri et al., 2002, 2003; Suzuki et al., 2005). Numerical solutions provided in particular a more detailed description of unstable column behavior (Neri and Dobran, 1994; Neri et al., 2002; Di Muro et al., 2004) in which the jet separates into a less dense part that forms a convective column and a denser part that collapses to produce pyroclastic flows. Thanks to the constant improvement of these models, in particular concerning the treatment of the solid phase modelled with one (Valentine and Wohletz, 1989), two (Neri and Macedonio, 1996) and N components (Neri et al., 2003), these numerical models can be used to assess volcanic eruption hazard (Todesco et al., 2002). However, because theses models are based on rather complex governing equations for multiphase flows, the interpretation of their outputs is not always straightforward. On the other hand, as simplified 1D models are based on rather stringent assumptions, they provide a useful tool to infer the level of complexity required to satisfyingly reproduce the behavior of natural flows.

The models based on simplified 1D formalism (Wilson, 1976; Sparks, 1986; Woods, 1988) stand as the most used method to estimate the source conditions of a Plinian eruption from its fallout deposits and the deduced height of the buoyant eruptive column from which they settled (Carey and Sparks, 1986; Koyaguchi and Ohno, 2001a). The predictions of 1D models for the behavior of buoyant Plinian columns are in agreement with numerical multiphase models (e.g. Dartevelle et al., 2004; Suzuki et al., 2005) which show that they encompass the major characteristics of the turbulent flow. On the other hand unsteady oscillations of volcanic jets, such as the one producing partial collapse (e.g. Di Muro et al., 2004) cannot be reproduced by 1D steady-state models. We will show here that 1D models currently used for buoyant Plinian plumes also failed the test of predicting quantitatively the onset of total column collapse according to field data.

The first goal of this paper is to establish a firm basis for confronting the predictions of models with the field data related to the onset of column collapse. We then propose an original improvement of the 1D model of the volcanic column incorporating a new theoretical description of turbulent entrainment. This model, based on independent laboratory experiments, is found to be in excellent agreement with field data and emphasizes the role of negative buoyancy in the generation of pyroclastic flows.

2. Physical model of an explosive eruption column

The dynamics of turbulent jets and plumes has been extensively studied since the 1950s. In their very influential study, Morton et al. (1956) proposed a comprehensive formalism to handle the turbulent behavior of such flows. They used a "top-hat" formalism in which all the dynamical variables are considered constant inside the flow and zero outside, which considerably simplifies calculations by reducing them to a one-dimensional evolution. The key physical hypothesis of their model is that the horizontal rate of entrainment of surrounding fluid is proportional to the local vertical ascension rate of the plume, via a constant coefficient α_e. This approach has been widely used in engineering and environmental fluid dynamics to study the motion of heated convective clouds or smoke issuing from industrial chimneys or from large-scale fires (e.g. Briggs, 1969; Fischer et al., 1979; Turner, 1986). Sparks (1986) and Carey and Sparks (1986)

Please cite this article as: Carazzo, G., et al., On the dynamics of volcanic columns: A comparison of field data with a new model of negatively buoyant jets, J. Volcanol. Geotherm. Res. (2008), doi:10.1016/j.jvolgeores.2008.01.002

adapted the top-hat formalism to volcanic plumes and introduced a theoretical model for the umbrella cloud in order to quantify the transport and the dispersion of lithic fragments as a function of the maximum height reached by the column. Their work provided a useful method to assess the mass flux of an eruption from the distribution of its deposits which is extensively used in field studies. Woods (1988) focused his study on the dynamics of the column itself and refined the model by introducing thermal effects and looking at their influence on the evolution of the bulk density of the flow.

2.1. Conservation laws

For a volcanic jet and a stratified environment, the three basic macroscopic conservation laws of volume, momentum and energy fluxes can be written as (Woods, 1988),

$$\frac{\mathrm{d}}{\mathrm{d}z}\left(\rho U R^2\right) = 2\rho_a U_\epsilon R \tag{1}$$

$$\frac{\mathrm{d}}{\mathrm{d}z}\left(\rho U^2 R^2\right) = g\ (\rho_a - \rho) R^2 \tag{2}$$

$$\frac{\mathrm{d}}{\mathrm{d}z}\left(\rho c_p T U R^2\right) = 2U_\epsilon R\left(c_a T_a + \frac{U^2}{2}\right) - \rho_a g U R^2 \tag{3}$$

with U the vertical velocity, R the jet radius, c_a, T_a and ρ_a the specific heat at constant pressure, the temperature and the density of the atmosphere, respectively, and c_p, T and ρ those of the bulk mixture. The top-hat entrainment coefficient α_e of Morton et al. (1956) defines the entrainment rate, $U_\epsilon = \alpha_e U$, which quantifies the rate of turbulent mixing of external air within the volcanic column. This set of equations is based on three main underlying assumptions: (1) the mixture of gas and volcanic fragments forming the column can be considered as a dusty gas with no mechanical and no thermal disequilibrium between the gas and the solids, (2) there is no significant pressure gradient between the core of the jet and the surrounding air at a given height, and (3) the flow is self-similar (the velocity and reduced gravity profiles keep a constant shape). This model will apply if the fragments are in majority small ash particles, which is the case for Plinian eruptions (Kaminski and Jaupart, 1998), and if there is no strong overpressure in the jet. This latter condition is however usually not fulfilled at the vent.

2.2. Exit conditions at the vent

The exit conditions at the vent, which are the initial conditions for the volcanic jet, depend indeed on the dynamics of the flow in the conduit. For typical values of volcanic mass flux and dissolved gas in the magma chamber, the volcanic mixture will exit the vent in "choked" conditions, i.e. at a sonic velocity, but with a larger pressure than the atmosphere (e.g. Woods and Bower, 1995; Papale et al., 1998). The first stage at the very base of the volcanic jet is thus a rapid decompression (and a strong acceleration of the mixture) to reach the atmospheric pressure. Because this evolution is rapid and induces the formation of a shock wave, entrainment is negligible during that stage (Kieffer and Sturtevant, 1984; Valentine and Wohletz, 1989; Dobran et al., 1993). After the decompression to 1 atm, the velocity of mixture is supersonic and can be expressed as (Woods and Bower, 1995)

$$U_v = 138\sqrt{n}, \tag{4}$$

for an average temperature of 1200 K, where n is the gas fraction in wt.%. We use this relationship between velocity and gas fraction as the initial condition for the 1D modeling, together with a prescribed mass flux (which itself is not affected by the initial decompression).

2.3. The bulk density

After the initial decompression, the mixture density is reduced both by dilution and heat exchanges between the hot pyroclasts and the cold atmospheric air engulfed. The ability of the column to form a Plinian plume thus depends on the amount of particles in the flow and the efficiency of heat exchanges as a function of the size of pyroclasts. For the small sizes assumed in Woods (1988), there is no mechanical or thermal desequilibrium between the phases and the following set of constitutive equations accounts for the influence of particle mass fraction on the bulk density,

$$\frac{1}{\rho} = \frac{(1-n)}{\rho_p} + \frac{nR_g T}{P} \tag{5}$$

$$n = 1 + (n_0 - 1)\frac{\rho_0 U_0 R_0^2}{\rho U R^2}, \tag{6}$$

$$R_\mathrm{g} = R_a + \left(R_{\mathrm{g}0} - R_a\right)\left(\frac{1-n}{n}\right)\left(\frac{n_0}{1-n_0}\right), \tag{7}$$

with n the gas mass fraction, R_g the bulk gas constant for the column, P the atmospheric pressure, and where the subscript 0 denotes a value at the source. At face value, the model given by Eqs. (1)–(7) gives access to the evolution of the mixture density, the velocity, the plume radius, and ultimately the eruptive regime as a function of α_e and vent conditions. For a given eruption, i.e. a given set of vent conditions, the choice of α_e will control the dynamics of the column.

2.4. The turbulent entrainment

The value of α_e has long been recognized as the key parameter of turbulent entrainment. Measurements were performed by numerous authors on turbulent jets with various specific source conditions representing end-member cases in fluid dynamics: pure jets (no initial buoyancy) and pure plumes (no initial inertia). These studies show that the value of α_e may vary considerably, from 0.07 for pure jets to 0.16 for pure plumes (Kaminski et al., 2005). In volcanology it has become common to take the value $\alpha_e = 0.1$. This choice may arguably be relevant in that it may be thought of as representing a mean value of α_e between a "jet" value for the inertia dominated region at the base of the column

Please cite this article as: Carazzo, G., et al., On the dynamics of volcanic columns: A comparison of field data with a new model of negatively buoyant jets, J. Volcanol. Geotherm. Res. (2008), doi:10.1016/j.jvolgeores.2008.01.002

and a "plume" value for the buoyancy dominated region above the point of buoyancy inversion. However there has been little analysis as to whether this value is really appropriate, i.e. whether quantitative predictions agree well with field observations.

3. The Plinian plume/pyroclastic fountain transition: observations and models

The dynamical behavior of a volcanic jet also strongly depends on the source conditions of the eruption. Theoretical models showed that the eruptive regime is governed by the initial radius, velocity and exsolved gas content. With a first aim of testing the theoretical predictions with field observations, we reviewed data available on a wide range of explosive eruptions. For most of the eruptions one can only assess the initial mass fraction of gas and the initial mass flux, but models of conduit flow (Wilson et al., 1980; Dobran, 1992; Papale et al., 1998; Papale and Polacci, 1999; Koyaguchi, 2005) can be used to define relationships between eruption velocity and mass fraction of gas reducing the number of source variables controlling the dynamical regime.

3.1. Geological parameters

The mass discharge rate feeding a Plinian column can be inferred from the height reached by the volcanic plume (e.g. Sparks, 1986) (Table 1). For recent eruptions, this height can be measured by satellite-based radar techniques (Holasek et al., 1996), whereas ancient eruptions require use of the method developed by Carey and Sparks (1986) based on the distribution of lithic material in the deposits around the vent. More elaborate models can be used to assess the height of the column from the fallout deposits (e.g. Koyaguchi and Ohno, 2001a). When both radar measurements and different methods can be used, they yield very similar results (Mount Saint-Helens (Carey et al., 1990), Pinatubo (Holasek et al., 1996; Koyaguchi and Ohno, 2001b)), with a difference of less than 8% between the estimated heights. As the eruptive mass flux scales as the fourth power of the height of the column (Sparks, 1986), the corresponding error on the mass flux is less than 33%. We use this value as the average error in the determination of the mass flux for the buoyant columns.

The estimation of the mass flux of collapsing fountains is not as straightforward. For the Krakatau eruption we used the total volume of pyroclasts emitted (Self and Rampino, 1981) and collected information on the time of the eruption given by witnesses (Carey et al., 1996). The resulting value, 2×10^9 kg s^{-1}, is close to the independent estimate of 3×10^9 kg s^{-1} by Legros and Druitt (2000) using a model of dense flow in water. Mass fluxes can also be estimated from the flow velocities inferred from the deposits (for example, for the Taupo ignimbrite (Wilson, 1985) or for the Katmai VTTS eruption (Fierstein and Hildreth, 1992)). In general however, mass discharge rates are calculated using the model of Bursik and Woods (1996) which estimate the mass flux from the run-out distance reached by the pyroclastic flows observed in the field. This model treats pyroclastic flows as dilute suspension, and there is some debate as to the validity of the formalism if the run-out distance is in fact controlled by the dense underflow that may form at the base of the suspension (see Druitt (1998) for a detailed discussion on the mode of emplacement of pyroclastic flows). There is no model that allows one to estimate the run-out distance of a dense current with a constant mass discharge rate. However, some recent experiments on the spreading of fluidized volcanic ash by Girolami et al. (in press) give some insight into the mobility of the flow as a function of its dilution. The Bursik and Woods' model considers typically a gas content between 10 and 30% in the flow. Girolami and coworkers' experiments show that the run-out distance for these gas contents is about twice as large than the run-out of a flow with the same mass (or same volume) but without gas. Fig. 5 of Bursik and Woods (1996) shows that the mass flux scales as the second power of the run-out distance. It will take thus a mass flux four times larger for a dense flow to reach the same distance as a dilute suspension. When only the run-out distance is known for a pyroclastic flow, we give in Table 2 both the minimum mass flux, calculated from Bursik and Woods (1996), and an estimated upper bound (four times larger) for a dense flow.

Initial amounts of gas in the eruptive mixture at the vent are more difficult to assess. One can determine the volatile concentration in the magma from melt inclusions (Rutherford et al., 1985). Assuming that water is the only gaseous phase in the magmatic melt, one can then estimate the initial bulk gas content

Table 1
Initial gas contents (n_0) corrected from observed lithics and crystals contents and total mass discharge rates (M) deduced from maximum heights (H) of Plinian phases of explosive eruptions. References: 1. Sigurdsson and Sparks (1980); 2. Sparks et al. (1991); 3. Bursik and Woods (1996); 4. Gardner et al. (1991); 5. Wallace et al. (1999); 6. Rosi et al. (1999); 7. Bohrson et al. (2006); 8. Carey and Sigurdsson (1989); 9. Luhr (1990); 10. Sigurdsson et al. (1987); 11. Varekamp et al. (1984); 12. Gardner et al. (1996); 13. Walker and Croasdale (1970); 14. Houghton et al. (2004); 15. Westrich et al. (1991); 16. Wehrmann (2005); 17. Bardintzeff et al. (1989); 18. Martel et al. (2000); 19. Carey et al. (1990); 20. Rutherford et al. (1985); 21. Carey and Sigurdsson (1985); 22. Naranjo et al. (1986); 23. Melson et al. (1990); 24. Wallace (2005); 25. Borisova et al. (2005); 26. Koyaguchi and Ohno (2001b); 27. Cas and Wright (1987); 28. Druitt et al. (1989); 29. Sparks and Wilson (1989); 30. Cottrel et al. (1999); 31. Wilson (1980); 32. Sigurdsson and Carey (1989); 33. Walker (1980); 34. Dunbar and Kyle (1993); 35. Carey and Sigurdsson (1987); 36. Sigurdsson et al. (1985); 37. Sigurdsson et al. (1990)

Eruption (deposit)	H (km)	M (kg/s)	n_0 (wt.%)	References
Askja (D)	26	$4.4\ 10^7$	2.9	(1,2)
Bishop Tuff (F7)	45	$4\ 10^8$	4.5	(3–5)
Campi Flegrei (V3)	44	$3.6\ 10^8$	2.2	(6–8)
El Chichon (C)	29	$6.8\ 10^7$	3.3	(9–11)
Fogo (A)	30	$7.8\ 10^7$	2.3	(12,13)
Katmai (CD)	25	$3.8\ 10^7$	1.8	(14,15)
Masaya (F)	20	$1.3\ 10^7$	0.8	(16)
Montagne Pelée (P1)	30	$7.8\ 10^7$	4.8	(17,18)
Mount St Helens (B4)	19	$1.3\ 10^7$	2.3	(19–21)
Nevado del Ruiz (1985)	27	$5.1\ 10^7$	1.3	(22–24)
Pinatubo (C1)	48	$5.1\ 10^8$	2.7	(25,26)
Santa Maria (1902)	34	$1.3\ 10^8$	1.7	(8,24,27)
Santorini (Minoan)	36	$1.6\ 10^8$	4.8	(28–31)
Tambora (F4)	44	$3.6\ 10^8$	2.0	(32)
Taupo	51	$6.5\ 10^8$	3.4	(3,33,34)
Vesuvius (W/G-S1)	32	$1\ 10^8$	2.2	(35–37)

Please cite this article as: Carazzo, G., et al., On the dynamics of volcanic columns: A comparison of field data with a new model of negatively buoyant jets, J. Volcanol. Geotherm. Res. (2008), doi:10.1016/j.jvolgeores.2008.01.002

Table 2
Initial gas contents (n_0) corrected from observed lithics and crystals contents and total mass discharge rates (M) for phases of collapse of explosive eruptions. References: 1. Aramaki (1984); 2. Aramaki and Ui (1966); 3. Bursik and Woods (1996); 4. Dunbar and Hervig (1992); 5. Turbeville and Self (1988); 6. Anderson et al. (1989); 7. Wilson and Hildreth (2003); 8. Rosi et al. (1996); 9. Signorelli et al. (1999); 10. Luhr (1990); 11. Sigurdsson et al. (1987); 12. Macias et al. (1998); 13. Westrich et al. (1991); 14. Fierstein and Hildreth (1992); 15. Self and Rampino (1981); 16. Carey et al. (1996); 17. Mandeville et al. (1996a); 18. Mandeville et al. (1996b); 19. Legros and Druitt (2000); 20. Rutherford et al. (1985); 21. Carey and Sigurdsson (1985); 22. Rowley et al. (1981); 23. Borisova et al. (2005); 24. Koyaguchi and Ohno (2001b); 25. Scott et al. (1991); 26. Cottrel et al. (1999); 27. Wilson (1980); 28. Bond and Sparks (1976); 29. Sigurdsson and Carey (1989); 30. Self et al. (1984); 31. Dunbar and Kyle (1993); 32. Walker and Wilson (1983)

Eruption (deposit)	Runout (km)	M (kg/s)	n_0 (wt.%)	References
Aira (Ito)	52	$1–4\ 10^{10}$	0.9	(1,2)
Bandelier (LBT)	30	$2.5–10\ 10^{9}$	1.3	(3–5)
Bishop Tuff	40	$5–20\ 10^{9}$	3.7	(3,6,7)
Campi Flegrei	63	$1.2–4.8\ 10^{10}$	0.4	(3,8,9)
El Chichon	6	$2–8\ 10^{8}$	1.2	(10–12)
Katmai (VTTS)	21	$5–20\ 10^{8}$	2.3	(3,13,14)
Krakatau (1883)	–	$1.2–3\ 10^{9}$	3.4	(15–19)
Mount St Helens (B3)	8	$3.5–14\ 10^{8}$	2.3	(3,20–22)
Pinatubo (C1)	13	$1.2–1.8\ 10^{9}$	2.7	(23–25)
Santorini (Minoan)	–	$1.2\ 10^{9}$	2.5	(26–28)
Tambora (F5/S1)	–	$5–14\ 10^{8}$	1.1	(29,30)
Taupo	80	$2–8\ 101^{0}$	3.3	(3,31,32)

in the eruption column by correcting the volatile concentration for the presence of crystals and lithics and assuming that all the volatiles are exsolved (Tables 1 and 2).

3.2. Predictions of the 2D/3D models

We used the field measurements reported in Tables 1 and 2 to test the column collapse predictions of the numerical simulations of 2D/3D models (Valentine and Wohletz, 1989; Neri and Dobran, 1994; Oberhuber et al., 1998; Suzuki et al., 2005). In their early study, Valentine and Wohletz (1989) proposed a 3D transitional diagram between the convective and the collapsing regimes as a function of three dimensionless parameters. Considering a freely decompressing jet at the same pressure as the atmosphere, one can extract from their surface defining the transition (in their Fig. 5) a single curve that we compare with field measurements (Fig. 2). Neri and Dobran (1994) and later Suzuki et al. (2005) proposed flow regime maps obtained by varying independently the exit velocity and the mass discharge rate for a given amount of gas at the source. Accounting for the relationship between gas mass fraction and the exit velocity (using Eq. 4), each of these transition curves corresponding to a given amount of gas at the source provides a point in Fig. 2. As illustrated by Fig. 2, this short review shows a disagreement between the numerical results and the field data. Only the most recent and accurate model (Suzuki et al., 2005) gives a consistent result. Suzuki et al. (2005) explained the variability of numerical results by differences in the parameterization chosen for the modeling of the turbulence (e.g. 2D vs 3D schemes, grid resolution, closure equations). Progress is being made in the development of this new generation of numerical models (Oberhuber et al., 1998; Neri et al., 2002; Suzuki et al., 2005), but as yet, there are no benchmark-type calculations that can clearly identify the origin (in the theoretical or in the numerical treatment of the multiphase flow) of the discrepancy amongst numerical models' predictions and between numerical model predictions and field data. On the other hand, top-hat 1D models provide a relatively simple basis for studying explosive volcanic jets, particularly for looking systematically at variations of behavior as a function of a given parameter or as a function of a specific ingredient added in the formalism. The

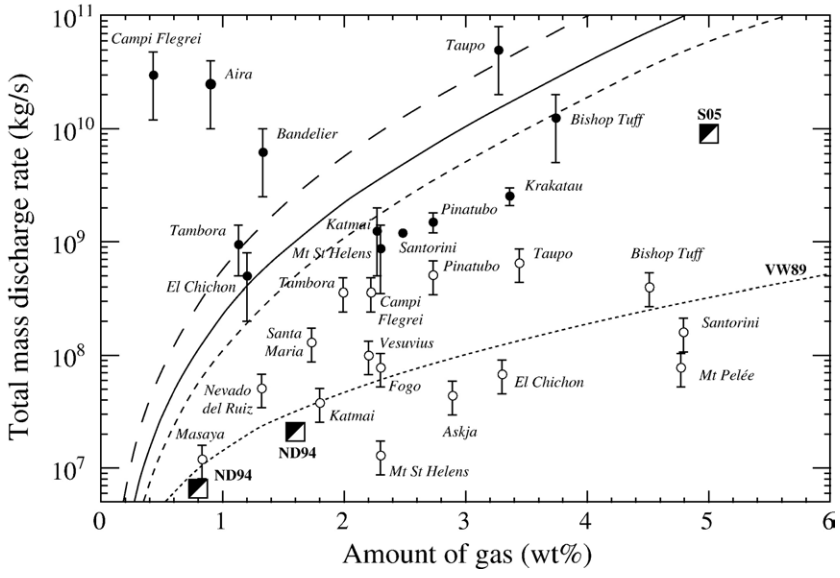

Fig. 2. Maximum initial mass flux (in kg/s) feeding a convective column eruption for a range of initial gas content (in wt.%) on an ensemble of well-studied historical eruptions. Solid circles represent mass fluxes deduced from deposits generated by collapsing fountain whereas open circles correspond to "Plinian" eruptions. Solid, large dashed and dashed lines gives the theoretical threshold for three values of α_e, 0.1, 0.07 and 0.16 respectively. Other symbols and line correspond to prediction of numerical models: VW89, Valentine and Wohletz (1989); ND94, Neri and Dobran (1994); S05, Suzuki et al. (2005).

Please cite this article as: Carazzo, G., et al., On the dynamics of volcanic columns: A comparison of field data with a new model of negatively buoyant jets, J. Volcanol. Geotherm. Res. (2008), doi:10.1016/j.jvolgeores.2008.01.002

question that we discuss here is whether we can build the necessary sophistication into the basically simple structure of such models to give them the power to quantitatively tackle the question of the onset of column collapse.

3.3. Prediction of classical 1D models

We also compared the field constraints with the theoretical predictions of the 1D model presented in Section 2. Fig. 2 shows that this 1D model does not achieve a good prediction of the transition between the buoyant and the collapsing regimes with respect to field data. Theoretical predictions using constant $\alpha_e=0.1$ systematically overestimate the critical mass flux by at least an order of magnitude which is much greater than the possible error on the data. The extension of the model to the extreme values of α_e that can be found in the experimental literature does not satisfactorily improve the predictions (Fig. 2). Consistency between field data and the 1D model could only be reached by strongly reducing α_e to values never found by experimental measurements in pure plumes and pure jets.

The choice of $\alpha_e=0.1$ appearing inconsistent with this aspect of field data, we first focus our attention on finding a more appropriate value for volcanic jets. If the poor performance of the standard model is to be attributed only to an incorrect value of α_e this field evidence strongly suggests that improved quantitative analysis of entrainment is required. A value of α_e can be inferred from specific field observations using appropriately the model framework described above. In a study of jets photographed at the Soufriere Hills Volcano, Formenti et al. (2003) used the heights reached by individual jets to constrain the value of α_e and found values as low as 0.01. This value is strikingly low but as we saw by confronting the predictions of the standard (constant α_e) model with field data from eruption deposits of a range of magnitudes, the basic result of low α_e is quite general. Hence it seems sensible to ask whether there is a reason why α_e should be much lower in volcanic jets than the values commonly cited in the fluid dynamics literature?

4. An alternative description of turbulent entrainment

4.1. Turbulent entrainment in jets with arbitrary buoyancy

Understanding the meaning of the different values of α_e measured in experimental jets and plumes has been a long standing open question in fluid mechanics. Some authors explained the larger entrainment observed in plumes than in jets by an effect of additional turbulence induced by positive buoyancy and proposed semi-empirical parameterizations of α_e to account for it (Wang and Law, 2002),

$$\alpha_e = \alpha_j + (\alpha_p - \alpha_j)\left(\frac{\mathrm{Fr}_p}{\mathrm{Fr}}\right)^2, \tag{8}$$

where α_j and α_p are the mean values of α_e for pure jets and pure plumes respectively, Fr is the Froude number which compares the inertia and buoyancy forces in the flow and Fr_p the Froude number for a pure plume. This equation indeed implies that positive buoyancy increases the turbulent entrainment. However such a parameterization is not based on physical considerations and does not account for the effect of negative buoyancy that is expected at the base of an explosive eruption column. With the aim of clarifying the physics behind this parameterization and proposing a universal expression for α_e, we built a new model that allows it to vary as local dynamic conditions evolve downstream from the source (Kaminski et al., 2005). Our theoretical framework has been validated by laboratory experiments and allowed us to reconcile the different values of α_e available in the experimental literature (Carazzo et al., 2006). For present purposes, we write,

$$\alpha_e = \frac{C}{2} + \left(1 - \frac{1}{A}\right)\mathrm{Ri} + \frac{R}{2}\frac{\mathrm{d}\ln A}{\mathrm{d}z} \tag{9}$$

where z is the distance from source, $\mathrm{Ri}=G'R/U^2$ is the local Richardson number, with $G'=g(\rho_a-\rho)/\rho_a$ the "top-hat" reduced gravity, R the "top-hat" plume radius and U the "top-hat" velocity. A and C are dimensionless coefficients that depend on the structure of the flow, in particular the shapes of the cross-stream profiles of velocity, reduced gravity and turbulent stress. For the simple case of Gaussian profiles for velocity and reduced gravity, A and C cal be rewritten as,

$$A = \frac{2}{3}\left(1+\lambda^2\right), \tag{10}$$

$$C = -6\left(1+\lambda^2\right)\int_0^\infty r^* \exp\left(-r^{*2}\right) j\left(r^*\right) dr^*, \tag{11}$$

where λ is the ratio of the characteristic ($1/e$) width of the buoyancy profile to that of the velocity profile and j is the turbulent shear stress profile. C represents the fraction of the total energy flux available for entrainment by turbulent shear stress, whereas A reflects the influence of the shape of the velocity and reduced gravity profiles on the transfer of gravitational energy to turbulent stress (Kaminski et al., 2005). Our analysis of the published experimental data suggests that C can be taken as a constant equal to 0.135. On the other hand, A varies from one flow to another and according to the distance from the source between the extreme values of 1.08 and 1.80 due to both evolution of the turbulent Prandtl number and of the shapes of the profiles (Carazzo et al., 2006).

Our formalism clarifies the relation between the turbulent entrainment and the available buoyancy quantified by the local Richardson number. At first order, this model predicts that an input of positive buoyancy in the jet promotes turbulence and allows better entrainment of surrounding fluid whereas negative buoyancy reduces it. A quantitative description of that physics requires knowledge of the values of A with the distance from the source. A large number of profile measurements have enabled us (Carazzo et al., 2006) to obtain good constraints on the evolution of A relatively far from the source ($z/D>10$) and validate the formalism expressed by Eq. (9). In the particular

Please cite this article as: Carazzo, G., et al., On the dynamics of volcanic columns: A comparison of field data with a new model of negatively buoyant jets, J. Volcanol. Geotherm. Res. (2008), doi:10.1016/j.jvolgeores.2008.01.002

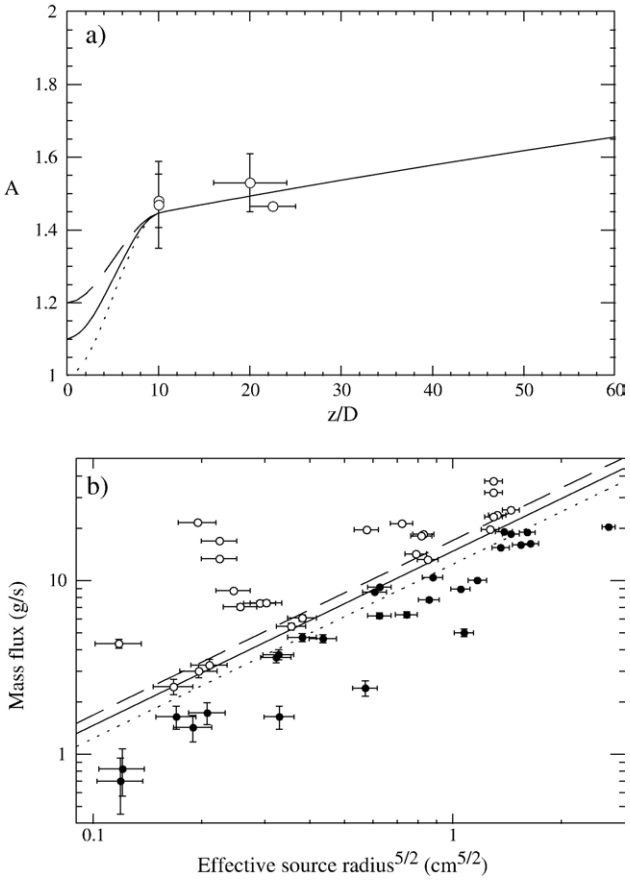

Fig. 3. (a) Evolution of A for negatively buoyant jets. Open circles represent experimental data (Keagy and Weller, 1949; Kiser, 1963; Uberoi and Garby, 1967) and the solid curve gives the evolution of A for momentum driven jets (no buoyancy) as a function of z/D the distance from the source (Carazzo et al., 2006) (D is the source diameter). Dotted, solid and dashed lines give the extrapolation to the source with $dA/dz=0$ and $A=1$, $A=1.1$ and $A=1.2$ at $z/D=0$, respectively. (b) Comparison between experiments and the prediction for the collapse of jets of EEG. Solid circles correspond to jets in the collapsing regime whereas open circles correspond to jets in the buoyant regime (Kaminski et al., 2005). The solid line gives the best fit, obtained with $A=1.1$ and $dA/dz=0$ at $z/D=0$.

case of explosive eruptions, the crucial effect enabling the volcanic jet to reach the Plinian regime is that enough air be entrained and heated close to the source to achieve a reversal of buoyancy before the initial momentum flux is exhausted. This raises the question of which value of A should be taken for negatively buoyant volcanic jets close to the source.

4.2. Experimental constraints

Experimental measurements on jets with negative buoyancy are quite sparse. Fig. 3a shows nevertheless that the few values available (Keagy and Weller, 1949; Kiser, 1963; Uberoi and Garby, 1967) collapse onto the universal curve of A obtained for pure momentum drivel jets (Carazzo et al., 2006). This result is consistent with the usual view of the base of an eruption column as a pure jet, although published models (Woods, 1995) do not allow for an effect of negative buoyancy on α_e. To complete the model, we need to extrapolate this curve to $z/D=0$, which we did by using a polynomial function for A (Fig. 3a),

$$A = a + b\left(\frac{z}{D}\right) + c\left(\frac{z}{D}\right)^2 d\left(\frac{z}{D}\right)^3, \quad (12)$$

where a, b, c and d are free coefficients. With the reasonable hypothesis $dA/dz=0$ (i.e. $b=0$) at the source and the continuity of A and dA/dz at $z/D=10$, the only unknown is the value of A at $z/D=0$ (i.e. a). To constrain the behavior of A near the source we use a set of experiments we have performed (Kaminski et al., 2005). Forced plumes with reversing buoyancy were generated by propelling a mixture of ethanol and ethylene glycol (EEG) into a tank of fresh water. EEG is less dense than water but an EEG-water mixture has the specific property to become denser because the evolution of density is a non-linear function of mixing ratio. Injected vertically downward, the jet naturally collapses to the top of the tank, but if entrainment is efficient enough the jet becomes heavier than its surroundings and forms a (negatively) buoyant plume. The experimental results were precise enough to determine a sharp limit between the buoyant and collapsing regimes. Our theoretical model produces an excellent fit to the data (Fig. 3b) which corresponds to $A=1.1$ (or $\lambda=0.65$) for $dA/dz=0$ at the source ($z/D=0$). We checked that the results were relatively insensitive to the condition on dA/dz at $z/D=0$.

The model described above has been developed for simple fluids, not for multiphase mixtures such as those involved in volcanic jets. It should apply to a volcanic jet only in the dusty gas approximation, i.e. only if one can neglect the effect of mechanical or thermal desequilibrium between the solid and the gas. The comparison of the new model predictions with field data will yield the answer to that question.

5. The Plinian/pyroclastic fountain transition revisited

5.1. Prediction of our model

As in Section 3.1 for the constant α_e models, the geological parameters are used to check the validity of our model. For this, we used the formalism expressed by Eqs. (1)–(4) and Eq. (9) to calculate α_e as a function of evolving Ri with $A=1.1$ and $dA/dz=0$ at ($z/D=0$). Fig. 4 shows that we achieve an excellent prediction of the transition between the buoyant and the collapsing regimes as constrained by field data.

The previously much worse prediction of transition flux obtained from constant entrainment models (also in Fig. 4) left open a legitimate question as to whether the discrepancy mainly reflected problems with the models or with the data themselves (Kaminski and Jaupart, 2001). Our result might be taken at face value to mean that the previous disagreement was a problem with the model, that is now resolved, but we now revisit this issue more carefully.

5.2. A test eruption: Mount Saint-Helens on 18 May 1980

Greater confidence in the consistency of our results can be obtained by testing the model on an eruption whose source

Please cite this article as: Carazzo, G., et al., On the dynamics of volcanic columns: A comparison of field data with a new model of negatively buoyant jets, J. Volcanol. Geotherm. Res. (2008), doi:10.1016/j.jvolgeores.2008.01.002

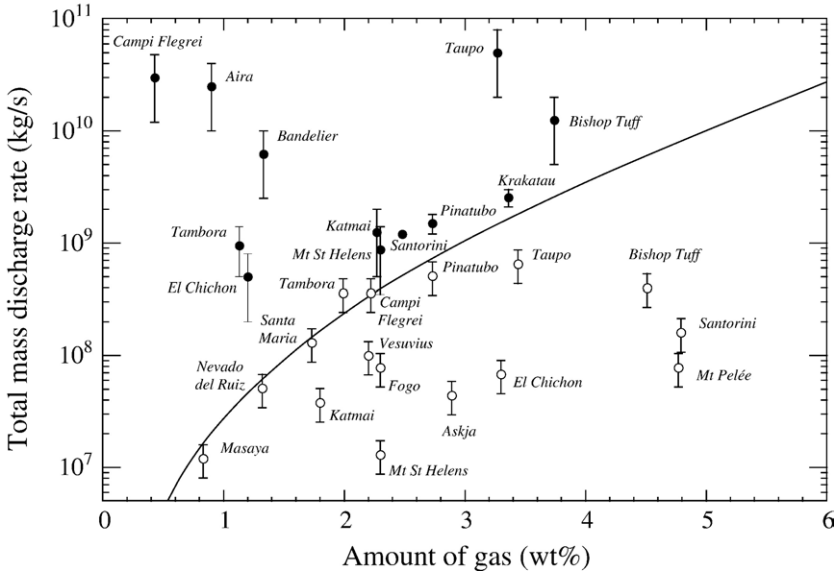

Fig. 4. Threshold mass discharge rate (in kg/s) between the collapsing and convecting regimes calculated as a function of gas content in the volcanic mixture (in wt.%) on an ensemble of well-studied historical eruptions. The symbols are the same than in Fig. 2. Solid line gives the theoretical threshold for our new model with variable α_e.

conditions are very well constrained. For this, we used a key example: the famous May 18, 1980 eruption of Mount Saint-Helens which was also carefully observed in real-time and hence for which durations of eruptive phases, deposit extent and volumes (Carey et al., 1990), and key magmatic properties (Rutherford et al., 1985) such as gas content and mixture temperature, are particularly well known. The buoyant column feeding the eruption cloud collapsed due to an increase of the mass flux and produced pyroclastic flows between 12:00 and 17:30 (Rowley et al., 1981). The source conditions of this eruption are input into the model to predict the critical mass discharge rate before the column collapses. This eruption was supersonic as suggested by the velocity determined from field studies (Carey and Sigurdsson, 1985). The bulk water content of the eruptive mixture has been taken equal to 2.3 wt.% after correcting for the measured crystal and lithic contents (Rutherford et al., 1985; Carey and Sigurdsson, 1985) and the temperature equal to 1200 K (Rutherford et al., 1985). Analyses of residual water contents in matrix glass suggest, as we assume, that all the volatiles were exsolved at fragmentation (Rutherford et al., 1985). We calculated the mass flux at column collapse from the pyroclastic flow run-out distance (Bursik and Woods, 1996), estimated at 8 km at Mount Saint-Helens (Rowley et al., 1981). Our estimations fall between 2.5 and 5 10^8 kg/s. By way of comparison, the peak mass discharge rate for the Plinian phase has been estimated at 1.6 10^7 kg/s from column height (Carey et al., 1990). Fig. 5 shows that our model provides a very satisfactory prediction with source conditions of the 1980 eruption. The Mount Saint-Helens eruption provides thus a very robust point of anchorage validating our model. The agreement between the model and such well known field data is in part dependent on the validity of the assumptions we made on the eruptive mixture. The accurate knowledge of the source conditions of this eruption is however unique and further discussion is required for other eruptions reported in this study.

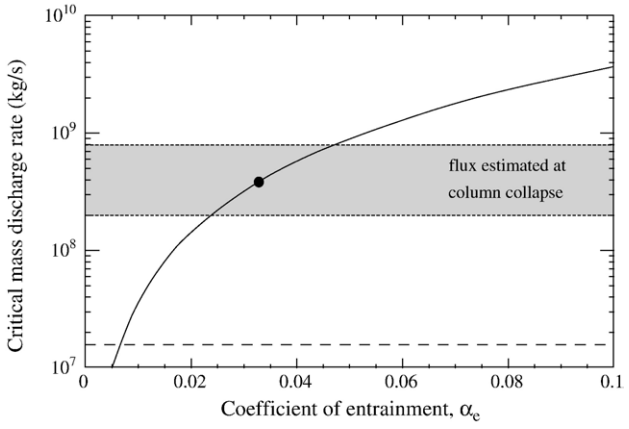

Fig. 5. Prediction of maximum mass discharge rate (in kg/s) feeding the eruption column before collapsing as a function of the coefficient of entrainment, α_e, for source conditions of the May, 18, 1980 eruption of Mount Saint-Helens (solid curve). Dashed line gives the peak mass flux estimated during the Plinian phase, whereas the grey area correspond to the flux estimated at column collapse. This flux implies a small entrainment (α_e=0.035). The solid circle represents the critical mass flux calculated with our model of reduction of entrainment due to negative buoyancy for this eruption.

6. Discussion

We have used a collection of field data on explosive volcanic eruptions in order to test the previous theoretical and numerical predictions of column collapse. We showed that the disagreement between the models and the geological evidence is corrected by accounting for the effect of negative buoyancy that strongly reduces the turbulent entrainment at the base of the column. The exact position of the threshold between the convective and the collapsing regimes in Fig. 4 depends however on the relationship between the exit velocity and the

Please cite this article as: Carazzo, G., et al., On the dynamics of volcanic columns: A comparison of field data with a new model of negatively buoyant jets, J. Volcanol. Geotherm. Res. (2008), doi:10.1016/j.jvolgeores.2008.01.002

gas content in the mixture we assumed. In spite of the lack of very well-studied eruptions that could give accurate information on the exit velocities, we investigate here the sensitivity of the prediction to the assumption made.

6.1. Subsonic/supersonic jets

The results presented above are valid for freely decompressing jets. Nevertheless, if the decompression occurs in a crater, the velocity is a complex function of the amount of gas, the mass discharge rate and the exit pressure of the flow (Woods and Bower, 1995). For low mass flux and low pressure, the jet becomes under-pressurized above the crater and issues at subsonic velocities. The jet is unable to reach the point of buoyancy inversion and the collapsing fountain regime dominates. This phenomenon may occur for small eruptions only and does not affect the powerful eruptions reported in this study ($>10^7$ kg/s).

If the initial mass flux and the exit pressure are high enough, the jet leaves the crater at supersonic velocity. Eruptions can occur with larger supersonic velocities if the conduit is sufficiently flared to form walls promoting the decompression and to allow a lithostatic pressure gradient in the flow (Wilson et al., 1980). Such conduit shapes may form after many hours of eruption and represent an upper bound. If one assumes that the pressure gradient was lithostatic for all the eruptions reported in Table 1, their transition curve (Fig. 4) would be shifted towards the field of collapsing fountains definitively disallowing agreement between the model at constant α_e ($0.07 \leq \alpha_e \leq 0.16$) and field data, but to a lesser extent our model also. A way to check the validity of the free-decompression hypothesis for all the eruptions reported in Table 1 lies in estimating exit velocities with an alternative method.

The method developed by Wilson (1976) to estimate the vent velocity of an eruption considers the equilibrium between the upward drag and downward gravity forces for a particle just before its fall. Under this condition, the momentum conservation law of the particle can be rewritten to provide the minimum velocity at the source needed to carry up the fragment issuing from the vent. An extrapolation of the maximum lithic size to the vent is needed to estimate the size of the largest fragments carried by the Plinian column. The resulting velocity strongly depends on this extrapolation, which ideally requires having numerous outcrops well distributed as a function of the distance from the source. We used isopleth maps from field studies to apply this method for some Plinian eruptions close to the collapsing threshold in Fig. 4. Our analysis shows that when the information on the distribution of the lithic sizes as a function of the distance from the source is well known (Plinian phases of Tambora, Taupo, Mount Saint-Helens, Montagne Pelée), the velocities coincide with the predictions of Eq. (4) (Fig. 6). For eruptions where the information is sparse (Plinian phases of Vesuvius, Campi Flegrei), the velocities calculated vary, probably due to errors in the extrapolation due to the lack of outcrops. It is possible that some eruptions reported here occurred in a flaring conduit, in particular the Santa Maria

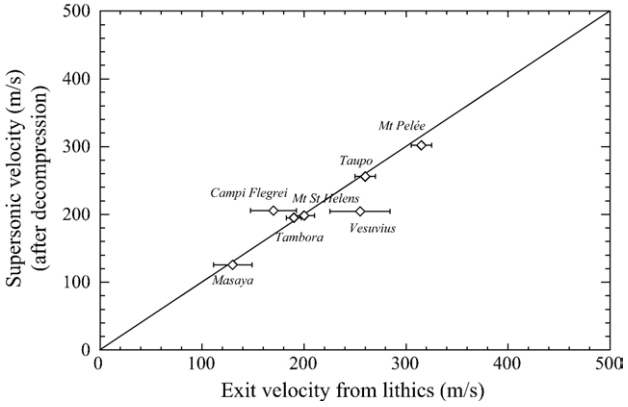

Fig. 6. Exit velocities measured with the method of Wilson (1976) (diamonds) as a function of the exit velocity predicted by Eq. (4) for 7 eruptions: Masaya: Wehrmann (2005); Tambora: Sigurdsson and Carey (1989); Mount St Helens: Carey and Sigurdsson (1985); Vesuvius: Sigurdsson et al. (1985); Campi Flegrei: Rosi et al. (1999); Taupo: Walker (1980); Mt. Pelée: Bardintzeff et al. (1989).

eruption where fragments of lithics up to 25 cm were found close to the vent (Williams and Self, 1983) or the Bishop Tuff eruption as suggested by estimations of decompression rates (Kaminski and Jaupart, 2001). These eruptions are therefore not so close to the transition as shown in Fig. 4 and provide less stringent constraints on a transition model.

6.2. Grain-size distributions

The amount of gas in the volcanic mixture has a large influence on the model prediction. The experimental measurements of volatile concentrations in melt inclusions may vary from one study to another because of differences between techniques, analytical difficulties or problems of selective preservation (Tait, 1992). Even for an eruption whose volatile content measurements agree, the effective gas mass fraction at the vent can diverge from the dissolved amount in the magma if (1) the exsolution is not complete or (2) if some gas is trapped by pumices due to low permeability (Kaminski and Jaupart, 1997). Kaminski and Jaupart (1998) showed that the gas entrapment is all the more important when pumices are large, i.e. that fragmentation is coarse. This effect is nevertheless difficult to quantify because it requires collecting accurate information on the source population of pumices and on the evolution of their permeability (Tait et al., 1998). The presence of large pumices in the eruptive mixture also strongly affects the dynamics of the column because they tend to retain their internal heat, limiting the capacity of the jet to develop a Plinian plume. Moreover, the sedimentation of the largest pumices changes the buoyancy of the jet. Both gas trapping and sedimentation effects modify thermal and momentum exchanges inside the plume.

The effect of thermal and mechanical disequilibrium has been studied by Woods and Bursik (1991) using 1D models. They showed that only thermal disequilibrium had implications for the behavior of the column but only if the grain-size distribution is coarse. In that case they predicted the formation of coarse-grained

Please cite this article as: Carazzo, G., et al., On the dynamics of volcanic columns: A comparison of field data with a new model of negatively buoyant jets, J. Volcanol. Geotherm. Res. (2008), doi:10.1016/j.jvolgeores.2008.01.002

cone forming fountains that do not produce pyroclastic flows. Numerical multiphase flows calculations (Valentine and Wohletz, 1989; Valentine et al., 1991; Neri and Dobran, 1994; Neri and Macedonio, 1996; Oberhuber et al., 1998; Neri et al., 2002, 2003; Suzuki et al., 2005) and laboratory experiments (Carey et al., 1988; Tait et al., 2006) will have to be performed to study in more detail the complex problem of the coupling between the grain-size distribution, the amount of gas released at fragmentation and the thermal and mechanical disequilibrium.

7. Conclusion

We used a new description of the turbulent entrainment to show the crucial effect of negative buoyancy in volcanic plumes. Its omission in the previous top-hat 1D models largely explains the discrepancy between the theoretical predictions and the constraints provided by field data. Our theoretical framework, which has been independently validated by laboratory experiments, achieved an excellent agreement with field data (Fig. 4). This strengthens considerably the quantitative relationship between model and the field data from eruption deposits, thereby increasing confidence in both. This may also show that a full modeling of the multiphase flow is not necessary to account for the collapse of the eruptive column. However, full 3-D multiphase numerical models are still required for the study of the partial collapse of volcanic jets.

New insights on the Plinian/pyroclastic flows transition could be brought by better constraining the velocities at the source and the effective gas content of the flow linked to the efficiency of fragmentation. Recent years have seen considerable advances in the technology permitting real-time observation of explosive eruptions by various remote-sensing methods (Seyfried and Hort, 1999; Donnadieu et al., 2005) and quantitative data on eruption cloud velocity, temperature, magmatic gas content and particle loading, for example, should eventually become available. Laboratory experiments and field studies on the onset of fragmentation (Gardner et al., 1996; Spieler et al., 2004; Koyaguchi, 2005) will also provide some answers to the problem of the effective amount of gas in the eruptive mixture at the vent.

Acknowledgments

The authors thank two anonymous reviewers and the associate editor, G. Valentine, for their fruitful comments. We also acknowledge L. Girolami for giving us access to her data. This work benefited from helpful discussions with T. Koyaguchi. Support was provided by the Institut National des Sciences de l'Univers (INSU-CNRS). This paper is IPGP contribution No. 2327.

References

Anderson, A.T., Newman, S., Williams, S.N., Druitt, T.H., Skirius, C., Stolper, E., 1989. H_2O, CO_2, Cl and gas in Plinian and ash-flow Bishop Tuff rhyolite. Geology 17, 221–225.

Aramaki, S., 1984. Formation of the Aira caldera, Southern Kyushu, 22,000 years ago. J. Geophys. Res. 89, 8485–8501.

Aramaki, S., Ui, T., 1966. The Aira and Ata pyroclastic flows and related caldera and depressions in Southern Kyushu, Japan. Bull. Volc. 29, 29–47.

Bardintzeff, J.M., Miskovsky, J.C., Traineau, H., Westercamp, D., 1989. The recent pumice eruptions of Mt. Pelée, Martinique. Part II: grain size studies and modelling the last Plinian phase P1. J. Volcanol. Geotherm. Res. 38, 35–48.

Bohrson, W.A., Spera, F., Fowler, S., Belkin, H., Vivo, B.D., Rolandi, G., 2006. Petrogenesis of the Campanian Ignimbrite: implications for crystals-melt separation and open-system processes from major and trace elements and Th isotopic data. Developments in Volcanology. Elsevier Press.

Bond, A., Sparks, R.S.J., 1976. The Minoan eruption of Santorini, Greece. J. Geol. Soc. Lond. 132, 1–16.

Borisova, A.Y., Pichavant, M., Beny, J.-M., Rouer, O., Pronost, J., 2005. Constraints on dacite magma degassing and regime of the June 15, 1991, climatic eruption of Mount Pinatubo (Philippines): new data on melt and crystal inclusions in quartz. J. Volcanol. Geotherm. Res. 145, 35–67.

Briggs, G.A., 1969. Optimum formulas for buoyant plume rise. Philos. Trans. R. Soc. Lond. 265, 197–203.

Bursik, M.I., Woods, A.W., 1996. The dynamics and thermodynamics of large ash flows. Bull. Volcanol. 58, 175–193.

Carazzo, G., Kaminski, E., Tait, S., 2006. The route to self-similarity in turbulent jets and plumes. J. Fluid. Mech. 547, 137–148.

Carey, S., Sigurdsson, H., 1985. The May 18, 1980 eruption of Mount St. Helens. 2. Modeling of dynamics of the Plinian phase. J. Geophys. Res. 90, 2948–2958.

Carey, S., Sparks, R.S.J., 1986. Quantitative models of the fallout and dispersal of tephra from volcanic eruption columns. Bull. Volcanol. 48, 109–125.

Carey, S., Sigurdsson, H., 1987. Temporal variations in column height and magma discharge rate during the 79 A.D. eruption of Vesuvius. Geol. Soc. Amer. Bull. 99, 303–314.

Carey, S., Sigurdsson, H., 1989. The intensity of Plinian eruptions. Bull. Volcanol. 51, 28–40.

Carey, S., Sigurdsson, H., Sparks, R.S.J., 1988. Experimental studies of particle-laden plumes. J. Geophys. Res. 93, 15,314–15,328.

Carey, S., Sigurdson, H., Gardner, J.E., Criswell, W., 1990. Variations in column height and magma discharge during the May 18, 1980 eruption of Mount St. Helens. J. Volcanol. Geotherm. Res. 43, 99–112.

Carey, S., Sigurdsson, H., Mandeville, C., Bronto, S., 1996. Pyroclastic flows and surges over water: an example from the 1883 Krakatau eruption. Bull. Volcanol. 57, 493–511.

Cas, R.A.F., Wright, J.V., 1987. Volcanic Successions: Modern and Ancient. Chapman and Hall, London. 528 pp.

Cottrel, E., Gardner, J.E., Rutherford, M.J., 1999. Petrologic and experimental evidence for the movement and heating of the pre-eruptive Minoan rhyodacite (Santorini, Greece). Contrib. Mineral. Petrol. 135, 315–331.

Dartevelle, S., Rose, W.I., Stix, J., Kelfoun, K., Vallance, J.W., 2004. Numerical modeling of geophysical granular flows: 2. Computer simulations of Plinian clouds and pyroclastic flows and surges. Geochem. Geophys. Geosyst. 5, (Q08004). doi:10.1029/2003GC000637.

Di Muro, A., Neri, A., Rosi, M., 2004. Contemporaneous convective and collapsing eruptive dynamics: the transitional regime of explosive eruptions. Geophys. Res. Lett. 31, L10607.

Dobran, F., 1992. Nonequilibrium flow in volcanic conduits and application to the eruptions of Mt. St. Helens on May 18, 1980, and Vesuvius in AD 79. J. Volcanol. Geotherm. Res. 49, 285–311.

Dobran, F., Neri, A., Macedonio, G., 1993. Numerical simulations of collapsing volcanic columns. J. Geophys. Res. 98, 4231–4259.

Donnadieu, F., Dubosclard, G., Cordesses, R., Allard, P., Druitt, T.H., Fournet-Fayard, J., Hervier, C., Kornprobst, J., Lénat, J.-F., Coltelli, M., 2005. Ground-based doppler radar monitoring provides new tool for the remote sounding of explosive volcanic activity. E.O.S. Trans. A.G.U. 86, 201–204.

Druitt, T.H., 1998. Pyroclastic density currents. In: Gilbert, J.S., Sparks, R.S.J. (Eds.), The Physics of Explosive Volcanic Eruptions. Geol. Soc. Lond. Spec. Pub., vol. 145, pp. 145–182.

Druitt, T.H., Melors, R.A., Pyle, D.M., Sparks, R.S.J., 1989. Explosive volcanism on Santorini, Greece. Geol. Mag. 126, 95–126.

Dunbar, N.W., Hervig, R.L., 1992. Volatile and trace element composition of melt inclusions from the Lower Bandelier Tuff: implications for magma chamber processes and eruptive style. J. Geophys. Res. 97, 15,151–15,170.

Please cite this article as: Carazzo, G., et al., On the dynamics of volcanic columns: A comparison of field data with a new model of negatively buoyant jets, J. Volcanol. Geotherm. Res. (2008), doi:10.1016/j.jvolgeores.2008.01.002

Dunbar, N.W., Kyle, P.R., 1993. Lack of volatile gradient in the Taupo Plinian-ignimbrite transition: evidence from melt inclusion analysis. Am. Mineral. 78, 612–618.

Fierstein, J., Hildreth, W., 1992. The Plinian eruptions of 1912 at Novarupta, Katmai National Park, Alaska. Bull. Volcanol. 54, 646–684.

Fischer, H.B., List, E.J., Koh, R.C.Y., Imberger, J., Brooks, N.H. (Eds.), 1979. Mixing in Inland and Coastal Waters. Academic, New-York.

Formenti, Y., Druitt, T.H., Kelfoun, K., 2003. Characterisation of the 1997 Vulcanian explosions of Soufrire Hills Volcano, Montserrat, by video analysis. Bull. Volcanol. 65, 587–605.

Gardner, J.E., Sigurdsson, H., Carey, S., 1991. Eruption dynamics and magma withdrawal during the Plinian phase of the Bishop Tuff eruption, Long Valley caldera. J. Geophys. Res. 96, 8097–8111.

Gardner, J.E., Thomas, R.M.E., Jaupart, C., Tait, S., 1996. Fragmentation of magma during Plinian volcanic eruptions. Bull. Volcanol. 58, 144–162.

Girolami, L., Druitt, T.H., Roche, O., Khrabrykh, Z., in press. Propagation and hindered settling of laboratory ash flows. J. Geophys. Res. doi:10.1029/2007JB005074.

Holasek, R.E., Self, S., Woods, A.W., 1996. Satellite observation and interpretation of the 1991 Mount Pinatubo eruption plumes. J. Geophys. Res. 101, 27,635–27,655.

Houghton, B.F., Wilson, C.J.N., Fierstein, J., Hildreth, W., 2004. Complex proximal deposition during the Plinian eruptions of 1912 at Novarupta, Alaska. J. Volcanol. Geotherm. Res. 66, 95–133.

Kaminski, E., Jaupart, C., 1997. Expansion and quenching of vesicular magma fragments in Plinian eruptions. J. Geophys. Res. 102, 12,187–12,203.

Kaminski, E., Jaupart, C., 1998. The size distribution of pyroclasts and the fragmentation sequence in explosive volcanic eruptions. J. Geophys. Res. 103, 29,759–29,779.

Kaminski, E., Jaupart, C., 2001. Marginal stability of atmospheric eruption columns and pyroclastic flow generation. J. Geophys. Res. 106, 21,785–21,798.

Kaminski, E., Tait, S., Carazzo, G., 2005. Turbulent entrainment in jets with arbitrary buoyancy. J. Fluid. Mech. 526, 361–376.

Keagy, W.R., Weller, A.E., 1949. A study of freely expanding inhomogeneous jets. Proc. Heat Transfer Fluid Mech. Inst. 2, 89–98.

Kieffer, S.W., Sturtevant, B., 1984. Laboratory studies of volcanic jets. J. Geophys. Res. 89, 8253–8268.

Kiser, K.M., 1963. Material and momentum transport in axisymmetric turbulent jets of water. A.I.Ch.E. J. 9, 386–390.

Koyaguchi, T., 2005. An analytical study for 1-dimensional steady flow in volcanic conduits. J. Volcanol. Geotherm. Res. 143, 29–52.

Koyaguchi, T., Ohno, M., 2001a. Reconstruction of eruption column dynamics on the basis of grain size of tephra fall deposits. 1. Methods. J. Geophys. Res. 106, 6499–6512.

Koyaguchi, T., Ohno, M., 2001b. Reconstruction of eruption column dynamics on the basis of grain size of tephra fall deposits. 2. Application to the Pinatubo 1991 eruption. J. Geophys. Res. 106, 6513–6533.

Legros, F., Druitt, T.H., 2000. On the emplacement of ignimbrite in shallow-marine environments. J. Volc. Geotherm. Res. 95, 9–22.

Luhr, J., 1990. Experimental phase relations of water- and sulfur-satured arc magmas and the 1982 eruptions of El Chichon volcano. J. Petrol. 31, 1071–1114.

Macias, J.L., Espindola, J.M., Bursik, M., Sheridan, M.F., 1998. Development of lithic-breccias in the 1982 pyroclastic flow deposits of El Chichon volcano, Mexico. J. Volcanol. Geotherm. Res. 83, 173–196.

Mandeville, C.W., Carey, S., Sigurdsson, H., 1996a. Magma mixing, fractional crystallization and volatile degassing during the 1883 eruption of Krakatau volcano, Indonesia. J. Volcanol. Geotherm. Res. 74, 243–274.

Mandeville, C.W., Carey, S., Sigurdsson, H., 1996b. Sedimentology of the Krakatau 1883 submarine pyroclastic deposits. Bull. Volcanol. 57, 512–529.

Martel, C., Bourdier, J.-L., Pichavant, M., Traineau, H., 2000. Textures, water content and degassing of silicic andesites from recent Plinian and dome-forming eruptions at Mt. Pelée volcano (Martinique, Lesser Antilles arc). J. Volcanol. Geotherm. Res. 96, 191–206.

Melson, W.G., Allan, J.F., Jerez, D.R., Nelen, J., Calvache, M.L., Williams, S.N., Fournelle, J., Perfit, M., 1990. Water contents, temperatures and diversity of the magmas of the catastrophic eruption of Nevado del Ruiz, Colombia, November 13, 1985. J. Volcanol. Geotherm. Res. 41, 97–126.

Morton, B.R., Taylor, G.I., Turner, J.S., 1956. Turbulent gravitational convection from maintained and instantaneous source. Proc. R. Soc. Lond. 234, 1–23.

Naranjo, J.L., Sigurdsson, H., Carey, S., Fritz, W., 1986. Eruption of the Nevado del Ruiz volcano, Colombia, on 13 November 1985: tephra fall and lahars. Science 233, 961–963.

Neri, A., Dobran, F., 1994. Influence of eruption parameters on the thermofluid dynamics of collapsing volcanic columns. J. Geophys. Res. 99, 11,833–11,857.

Neri, A., Macedonio, G., 1996. Numerical simulation of collapsing volcanic columns with particles of two sizes. J. Geophys. Res. 101, 8153–8174.

Neri, A., Di Muro, A., Rosi, M., 2002. Mass partition during collapsing and transitional columns by using numerical simulations. J. Volcanol. Geotherm. Res. 115, 1–18.

Neri, A., Esposti Ogaro, T., Macedonio, G., Gidaspow, D., 2003. Multiparticle simulation of collapsing volcanic columns and pyroclastic flow. J. Geophys. Res. 108. doi:10.1029/2001JB000508.

Newhall, C.G., Punongbayan, R.S. (Eds.), 1991. Fire and Mud. Eruptions and Lahars of Mt. Pinatubo, Philippines. University of Washington Press, Seattle.

Oberhuber, J.M., Herzog, M., Graf, H.-F., Schwanke, K., 1998. Volcanic plume simulation on large scales. J. Volcanol. Geotherm. Res. 87, 29–53.

Papale, P., Polacci, M., 1999. Role of carbon dioxide in the dynamics of magma ascent in explosive eruptions. Bull. Volcanol. 60, 583–594.

Papale, P., Neri, A., Macedonio, G., 1998. The role of magma composition and water content in explosive eruptions 1. Conduit ascent dynamics. J. Volcanol. Geotherm. Res. 87, 75–93.

Rosi, M., Vezzoli, L., Aleotti, P., Censi, M.D., 1996. Interaction between caldera collapse and eruptive dynamics during the Campanian Ignimbrite eruption, Phlegraean Fields, Italy. Bull. Volcanol. 57, 541–554.

Rosi, M., Vezzoli, L., Castelmenzano, A., Grieco, G., 1999. Plinian pumice fall deposit of the Campanian Ignimbrite eruption (Phlegraean Fields, Italy). J. Volcanol. Geotherm. Res. 91, 179–198.

Rowley, P.D.M.A., Kuntz, M., Macleod, N.S., 1981. Pyroclastic flow deposits in the 1980 eruptions of Mount St. Helens, Washington. U.S.G.S Prof. Paper 1250, 489–512.

Rutherford, M., Sigurdsson, H., Carey, S., Davis, A., 1985. The May 18, 1980 eruption of Mount St. Helens. 1. Melt composition and experimental phase equilibria. J. Geophys. Res. 90, 2929–2947.

Scott, W.E., Hoblitt, R.P., Torres, R.C., Self, S., Martinez, M.L., Nillos, T., 1991. Pyroclastic flows of the June 15, 1991, climatic eruption, of Mount Pinatubo. University of Washington Press, Seattle, in Fire and Mud. Eruptions and lahars of Mt. Pinatubo, Philippines.

Self, S., Rampino, M.R., 1981. The 1883 eruption of Krakatau. Nature 294, 699–704.

Self, S., Rampino, M.R., Newton, M.S., Wolff, J.A., 1984. Volcanological study of the great Tambora eruption of 1815. Geology 12, 659–663.

Seyfried, R., Hort, M., 1999. Continuous monitoring of volcanic eruption dynamics: a review of various techniques and new results from a frequency-modulated radar Doppler system. Bull. Volcanol. 60, 627–639.

Signorelli, S., Vaggelli, G., Romano, C., Carroll, M.R., 1999. Volatile element zonation in Campanian Ignimbrite magmas (Phlegraean Fields, Italy): evidence from the study of glass inclusions and matrix glasses. Contrib. Mineral. Petrol. 140, 543–553.

Sigurdsson, H., Sparks, R.S.J., 1980. Petrology of rhyolitic and mixed magma ejecta from the 1875 eruption of Askja, Iceland. J. Petro. 22, 41–84.

Sigurdsson, H., Carey, S., 1989. Plinian and co-ignimbrite tephra fall from the 1815 eruption of Tambora volcano. Bull. Volcanol. 51, 243–270.

Sigurdsson, H., Carey, S., Cornell, W., Pescatore, T., 1985. The eruption of Vesuvius in AD 79. Nat. Geogr. Res. 1, 332–387.

Sigurdsson, H., Carey, S., Fisher, R.V., 1987. The 1982 eruption of El Chichon volcano, Mexico (3): physical properties of pyroclastic surges. Bull. Volcanol. 49, 467–488.

Sigurdsson, H., Cornell, W., Carey, S., 1990. Influence of magma withdrawal on compositional gradients during the AD 79 Vesuvius eruption. Nature 345, 519–521.

Sparks, R.S.J., 1986. The dimensions and dynamics of volcanic eruption columns. Bull. Volcanol. 48, 3–15.

Sparks, R.S.J., Wilson, L., 1976. A model for the formation of ignimbrite by gravitational column collapse. J. Geol. Soc. Lond. 132, 441–451.

Please cite this article as: Carazzo, G., et al., On the dynamics of volcanic columns: A comparison of field data with a new model of negatively buoyant jets, J. Volcanol. Geotherm. Res. (2008), doi:10.1016/j.jvolgeores.2008.01.002

Sparks, R.S.J., Walker, G.P.L., 1977. Significance of vitric-enriched air-fall ashes associated with crystal-enriched ignimbrites. J. Volcanol. Geotherm. Res. 2, 329–341.

Sparks, R.S.J., Wilson, L., 1989. The Minoan Deposits: A Review of Their Characteristics and Interpretation. Thera and the Aegean World III, London.

Sparks, R.S.J., Wilson, L., Sigurdsson, H., 1991. The pyroclastic deposits of the 1875 eruption of Askja, Iceland. Philos. Trans. R. Soc. Lond. 299, 241–273.

Spieler, O., Kennedy, B., Kueppers, U., Dingwell, D.B., Scheu, B., Taddeucci, J., 2004. The fragmentation threshold of pyroclastic rocks. Earth Planet. Sci. Lett. 226, 139–148.

Suzuki, Y.J., Koyaguchi, T., Ogawa, M., Hachisu, I., 2005. A numerical study of turbulent behavior in eruption clouds using a 3-D fluid-dynamics model. J. Geophys. Res. 110, B08201.

Tait, S., 1992. Selective preservation of melt inclusions in igneous phenocrysts. Am. Min. 77, 146–155.

Tait, S., Thomas, R., Gardner, J., Jaupart, C., 1998. Constraints on cooling rates and permeabilities of pumice in an explosive eruption jet from colour and magnetic mineralogy. J. Volcanol. Geotherm. Res. 86, 79–91.

Tait, S., Carazzo, G., Kaminski, E., 2006. An experimental study of jets with reversing buoyancy with application to the partial collapse regime of explosive volcanic eruptions. EOS Trans. Am. Geophys. Union 87 V43C–1820.

Todesco, M., Neri, A., Esposti Ongaro, T., Papale, P., Macedonio, G., Scantacroce, R., Longo, A., 2002. Pyroclastic flow hazard assessment at Vesuvius (Italy) by using numerical modeling. I. Large-scale dynamics. Bull. Volcanol. 64, 155–177.

Turbeville, B.N., Self, S., 1988. San Diego Canyon ignimbrites: Pre-Bandelier tuff explosive rhyolitic volcanism in the Jemez Mountains, New Mexico. J. Geophys. Res. 93, 6148–6156.

Turner, J.S., 1986. Turbulent entrainment: the development of the entrainment assumption, and its application to geophysical flows. J. Fluid. Mech. 173, 431–471.

Uberoi, M.S., Garby, L.C., 1967. Effect of density gradients on an air jet. Phys. Fluids 10, 200–202.

Valentine, G.A., Wohletz, K.H., 1989. Numerical models of Plinian eruption columns and pyroclastic flows. J. Geophys. Res. 94, 1867–1887.

Valentine, G.A., Wohletz, K.H., Kieffer, S.W., 1991. Sources of unsteady column dynamics in pyroclastic flow eruptions. J. Geophys. Res. 96, 21,887–21,892.

Varekamp, J.C., Luhr, J.F., Prestegaard, K.L., 1984. The 1982 eruption of El Chichon volcano (Chiapas, Mexico): character of the eruptions, ash-fall deposits and gas phase. J. Volcanol. Geotherm. Res. 23, 39–68.

Walker, G.P.L., 1980. The Taupo pumice: product of the most powerful known (ultraplinian) eruption. J. Volcanol. Geotherm. Res. 8, 69–94.

Walker, G.P.L., Croasdale, R., 1970. Two Plinian type eruptions in the Azores. J. Geol. Soc. Lond. 127, 17–55.

Walker, G.P.L., Wilson, C.J.N., 1983. Lateral variations in the Taupo ignimbrite. J. Volcanol. Geotherm. Res. 18, 117–133.

Wallace, P.J., 2005. Volatiles in subduction zone magmas: concentrations and fluxes based on melt inclusion and volcanic gas data. J. Volcanol. Geotherm. Res. 140, 217–240.

Wallace, P.J., Anderson, A.T., Davis, A.M., 1999. Gradients in H_2O, CO_2 and exsolved gas in a large-volume silicic magma system: interpreting the record preserved in melt inclusions from the Bishop Tuff. J. Geophys. Res. 104, 20,097–20,122.

Wang, H., Law, A.W.-K., 2002. Second-order integral model for a round turbulent buoyant jet. J. Fluid. Mech. 459, 397–428.

Wehrmann, H., 2005. Volatile degassing and Plinian eruption dynamics of the mafic Fontana Tephra, Nicaragua. Ph.D. thesis, Kiel University.

Westrich, H.R., Eichelberger, J.C., Hervig, R.L., 1991. Degassing of the 1912 Katmai magmas. Geophys. Res. Lett. 18, 1561–1564.

Williams, S.N., Self, S., 1983. The October 1902 Plinian eruption of Santa Maria volcano, Guatemala. J. Volcanol. Geotherm. Res. 16, 33–56.

Wilson, L., 1976. Explosive volcanic eruptions-III. Plinian eruption columns. J. R. Astrom. Soc. 45, 543–556.

Wilson, L., 1980. Energetics of the Minoan Eruption: Some Revisions. Thera and the Aegeal World II, London.

Wilson, C.J.N., 1985. The Taupo eruption, New Zealand II. The Taupo ignimbrite. Philos. Trans. R. Soc. Lond. 314 (1529), 199–310.

Wilson, C.J.N., Hildreth, W., 2003. Assembling an ignimbrite: mechanical and thermal building blocks in the Bishop Tuff, California. J. Geol. 111, 653–670.

Wilson, L., Sparks, R.S.J., Walker, G.P.L., 1980. Explosive volcanic eruptions-IV. The control of magma properties and conduit geometry on eruption column behaviour. Geophys. J. R. Astrom. Soc. 63, 117–148.

Woods, A.W., 1988. The fluid dynamics and thermodynamics of eruption columns. Bull. Volcanol. 50, 169–193.

Woods, A.W., 1995. The dynamics of explosive volcanic eruptions. Rev. Geophys. 33, 495–530.

Woods, A.W., Bursik, M., 1991. Particle fallout, thermal disequilibrium and volcanic plumes. Bull. Volcanol. 53, 559–570.

Woods, A.W., Caulfield, C.P., 1992. A laboratory study of explosive volcanic eruptions. J. Geophys. Res. 97, 6699–6712.

Woods, A.W., Bursik, M., 1994. A laboratory study of ash flows. J. Geophys. Res. 99, 4375–4394.

Woods, A.W., Bower, S.M., 1995. The decompression of volcanic jets in a crater during explosive volcanic eruptions. Earth Planet. Sci. Lett. 131, 189–205.

Please cite this article as: Carazzo, G., et al., On the dynamics of volcanic columns: A comparison of field data with a new model of negatively buoyant jets, J. Volcanol. Geotherm. Res. (2008), doi:10.1016/j.jvolgeores.2008.01.002